High-performance rectifiers fabricated on a flexible substrate

D. Etor, L. E. Dodd, D. Wood and C. Balocco

School of Engineering and Computing Sciences, Durham University,

South Road, Durham, DH1 3LE, United Kingdom

ABSTRACT

We report on the fabrication and testing of metal-insulator-metal (MIM) diodes on a flexible substrate where the thin insulating layer self-assembles as a monolayer sandwiched between the two metal electrodes. The current-voltage characteristic has a strong asymmetry and non-linearity at zero-bias. The diodes have a typical zero-bias resistance of 80 kΩ, zero-bias curvature coefficient of 5.5 V^{-1} and voltage responsivity of 3.1 kV/W at a frequency of 1 GHz. The fabrication yield was over 90%, and an encapsulation method to prevent MIM junctions degradation has also been developed. The diodes show no significant degradation in performance when the substrate is stressed in a one-off bending experiment, although extensive testing does produce some loss in quality. The fabrication process is simple, cost effective and carried out at low temperature, opening up the possibility of roll-to-roll volume manufacturing of fast MIM diodes.

KEYWORDS: metal-insulator-metal diode, self-assembled monolayer, octadecyltrichlorosilane, molecular rectifier, microwave diode.

MAIN TEXT

The metal-insulator-metal (MIM) diode is a high-speed rectifier capable of operating at frequencies well into the infrared range.[1–5] The device consists of a thin dielectric layer (a few nanometers thick) sandwiched between two metal electrodes, with current flowing between the electrodes depending on the bias voltage polarity.

The main challenge in the fabrication of MIM diodes is the conformal dielectric deposition: a very thin dielectric layer has to be used, usually between 1 and 4 nm, corresponding only to a few atomic layers. This often results in a defective layer, with a large number of pin holes, which short-circuit the diode terminals and drastically reduce yield. To overcome this problem, we have previously reported the development of a MIM diode in which organometallic molecules self-assemble in an insulating monolayer.[6] The diode used an octadecyltrichlorosilane (OTS) self-assembled monolayer (SAM), which consists of carbon chains strongly packed together with an overall thickness of approximately 2 nm. Due to the nature of self-assembly, a second layer cannot grow on top of the first one, resulting in a uniform thickness over large areas determined by the SAM chemistry.[7,8] The fabrication process and materials are environmentally friendly, and they are also compatible with large-area roll-to-roll manufacturing. There is a lot of interest in this (flexible plastic substrates) technology [9–13] due to the distinct advantages it presents over the rigid substrates in many applications. Unlike the rigid substrates, the flexible plastic substrate is usually more robust and compact, has lighter weight, and is more cost effective.[9] The use of the plastic substrates has also enable new product concepts such as conformable sensors and curved displays.[9,13] While flexible devices such as organic diodes already exist, they are limited by poor frequency response.[14] This makes MIM diodes on flexible substrates very attractive due to their potential to operate at very high frequencies.

In this work, polyimide (PI) has been used to form a flexible substrate upon which Ti/OTS/Pt MIM diodes with a nominal junction area of 10 µm x 10 µm were fabricated. Polyimide is a high molecular weight and fully aromatic material, which is formed from polyamic acid precursors dissolved in an N-

methyl-2-pyrrolidone based solvent carrier: the material is mechanically robust, enabling thin layers to be formed, and can be spin coated over a large area.[15] Our MIM structures are therefore suitable for applications where a large area and a low manufacturing cost are of paramount importance, such as radio-frequency identification (RFID) tags operating at 980 MHz,[16–19] and energy harvesting if the structure dimensions are further optimised.[20–22]

A 2 inch diameter silicon wafer was used as a carrier for the polyimide substrate. Prior to the polyimide deposition, the silicon wafer was cleaned using a piranha solution (H_2SO_4:H_2O_2), and dried using N_2, followed by a bake at 200 °C for 3 minutes to dehydrate the surface. The polyimide was spin coated on the silicon wafer at 500 rpm for 10 seconds, and then 2000 rpm for 30 seconds, resulting in a   2.5 μm thick substrate. In order to be able to peel the substrate off the silicon carrier wafer without damage, the spin coating process was repeated two further times with a 5 minutes bake at 85 °C between each run, resulting in a total substrate thickness of 7.5 μm. After the final coating, the polyimide was part-cured by baking at 150 °C for 15 minutes, and fully cured in a convection oven at 350 °C with a ramp rate of 2 °C per minute. Higher ramp rates were found to cause bubbles within the polyimide, reducing yield.

After spin-coating the PI on the carrier wafer, the MIM structures were produced by depositing approximately 25 nm of titanium by e-beam evaporation. The titanium was then coated with OTS followed by the deposition of a layer of platinum with a thickness of approximately 40 nm by e-beam evaporation, resulting in the Ti/OTS/Pt junctions. The detail fabrication process and OTS deposition can be found elsewhere.[6] In order to improve the Ti film adhesion, the PI surface was activated in an O_2 plasma for 1 minute, with a pressure of 150 mT, an O_2 flow rate of 50 sccm, and an RF power of 75 W.

Following the completion of the MIM structures, the PI substrate was peeled off the carrier wafer. Current-voltage (*J-V*) characteristics were measured on the devices before (with over 90% device yield) and after peeling off the PI substrate. There was no loss of yield after the peeling process.

Figure 1 shows a picture of the completed devices and an AFM image of one of the structures, where the MIM junction is defined at the cross-over.

DC electrical characterization was carried out on the diodes using a parameter analyser. The diodes were tested over a voltage range of ±0.2 V in order to avoid damaging their junctions, as they were found to have an irreversible breakdown voltage of approximately ±0.35 V. A typical *J-V* characteristic is plotted in the inset of Fig. 2, showing a strong asymmetry and non-linearity at zero-bias. The zero-bias curvature coefficient (γ_{ZB}), as defined by Eq. (1), was found to be approximately 5.5 V^{-1} (see graph in Fig. 2), which is consistent with our previous results for devices fabricated on a glass substrate.[6]

$$\gamma_{ZB} = \left. \frac{d^2 I}{dV^2} \middle/ \frac{dI}{dV} \right|_{V=0} \tag{1}$$

where γ_{ZB} is the zero-bias curvature coefficient, $\left(\frac{dI}{dV}\right)^{-1}$ is the diode differential resistance, and *V* is the applied voltage.

The diodes' zero-bias resistance was approximately 80 kΩ (see Fig. 2), which is also consistent with our previous results,[6] and is considerably smaller than the values reported in the literature (typically in the MΩ regime).[23] The relatively small resistance associated with the diodes is attributed to the very thin OTS layer (~2 nm), as the resistance of MIM structures is significantly influenced by the thickness of the dielectric layer.[21] The lower resistance also improves the match of an antenna (with an impedance typically of the order of 100 Ω) to the didoes, thus improving the overall efficiency where the diode is used as a rectifier in rectenna devices.

To enable RF testing, ten diodes were embedded within a coplanar waveguide with a characteristic impedance of 50 Ω,[6] to minimize unwanted reflections from the layout as well as to reduce radiation losses. RF measurements on the diodes were carried out from 1 MHz to 3 GHz. The input RF power was compensated at different frequencies to account for the measured losses in the cables, probes and coplanar waveguides. The rectified output voltage was measured for RF input powers ranging from

20 nW to 500 nW (i.e. -47 dBm to -33 dBm). There was no light dependence observed on the device during the measurements, which were carried out at room temperature.

Figure 3(a) shows a typical rectified output voltage of the diode as a function of RF power fed into the coplanar waveguide at a frequency of 1 GHz. Fig. 3(b) shows the frequency response of the diode, measured up to 3 GHz with a constant input RF power of approximately 100 nW (-40 dBm).

The diode voltage responsivity R_v is defined as:

$$R_v = \frac{V_{OUT}}{P_{RF}} = \frac{d^2V}{dI^2} \Big/ \frac{dV}{dI} \qquad (2)$$

where V_{OUT} is the rectified voltage and P_{RF} is the RF power fed into the coplanar waveguide. Its value was determined by a linear fitting of the rectified output voltage as a function of the input RF power, shown in Fig. 3(a), and had an absolute value of approximately 3 kV/W at a frequency of 1 GHz.

The parameters which influenced the diode response were determined by measuring the reflection coefficient of the whole structure, s_{11}, as a function of the operating frequency using a vector network analyzer (VNA) and converting it into the input impedance Z_{IN}:[24]

$$Z_{IN} = Z_0 \left(\frac{1+s_{11}}{1-s_{11}} \right) \qquad (3)$$

where $Z_0 = 50\ \Omega$ is the characteristic impedance of the microwave probes and VNA ports. Z_{IN} was then fitted numerically [6], resulting in a series resistance $R_S = 34\ \Omega$ and a parallel capacitance $C_P = 2.9$ pF.

The diodes' zero-bias resistance was found to increase with time after fabrication, causing the rectified current to degrade, which is a typical problem associated with MIM junctions.[25] The issue was thought to be caused by the atmosphere (water vapour and oxygen) penetrating through the junction and oxidizing the Ti layer. We therefore fabricated MIM diodes on two separate wafers simultaneously under the same process conditions. Immediately after carrying out the first set of *J-V* measurements, one wafer was kept in an environment with normal atmospheric conditions (temperature of 20 °C and humidity of 48%), whilst the other was kept in vacuum. *J-V* measurements

were then repeated on the two sets of diodes daily for 3 weeks. Figure 4 shows the typical current degradation pattern of the diodes kept in normal atmosphere. As it can be seen, the rectified current degrades by approximately 75% within the first 150 hours following fabrication, and then stabilizes afterwards. The devices kept in vacuum degraded only by approximately 2% within the first 24 hours and remained stable thereafter.

Freshly fabricated devices were encapsulated in an epoxy resin, DELO, often used in the encapsulation of micro electro-mechanical systems (MEMS). The resin is highly stress-relieving and is flexible.[26–27] As it can be seen in the inset of Fig. 4, the diode leads and junctions were completely covered by the resin, exposing only the contact pads to allow electrical measurements to be performed. The results for the encapsulated devices are plotted in Fig. 4. Similar to the devices kept in vacuum, only a negligible amount of current degradation (approximately 2%) was observed, showing that the encapsulation method was very effective.

The device was tested while the substrate was wrapped on a disc shape metal rod. The device curvature coefficient was unaffected with a curvature (bend) radius of 4 cm, but started to degrade as the curvature radius decreased, as can be seen in Fig. 5. Although the device electrical parameters degrade while curved at these radii, the amount of degradation was insignificant. To further stress the device, the substrate was bent repeatedly using a cam shaft with a 1.5 cm stroke, driven by a motor with a constant speed of 60 rpm. The bend cycle was repeated 15000 times, with tests performed in between. In the inset of Fig. 5 is the plot of the device curvature coefficient and resistance as a function of the number of bend cycles. As can be seen, the device curvature coefficient had degraded by approximately 50% on completion of the test. This means that the device in its current form is more suitable for applications where constant and heavy vibration is not present.

In conclusion, MIM diodes have been fabricated on a thin, flexible polyimide substrate, with over 90% device yield. The diodes' insulating layer consisted of OTS, with the deposition process being carried out entirely at low temperature. The fabrication details presented here show that a roll-to-roll manufacturing process for MIM diodes is feasible. DC and RF analysis showed that the diodes had a

strong non-linear *J-V* characteristic with consistent typical zero-bias curvature coefficient of ~5.5 V^{-1} and a voltage responsivity of 3.1 kV/W at a frequency of 1 GHz. The diodes' rectified current were effectively prevented from degrading by encapsulating them in a flexible epoxy resin. The developed rectifiers are suitable for applications such as 13.6 MHz and 980 MHz RFID tags, as the devices are fast and have been fabricated on a thin 7.5 µm flexible substrate.

ACKNOWLEDGEMENT

REFERENCES

[1] E. Sakuma, and K. M. Evenson, IEEE J. Quant. Electron. **QE-IO**, 600 (1974).

[2] K. M. Evenson, J. S. Wells, L. M. Matarrese, and L. B. Elwell, Appl. Phys. Lett. **16**, 159 (1970).

[3] R. E. Drullinger, K. M. Evenson, D. A. Jennings, F. R. Petersen, J. C. Bergquist, L. Burkins, and H.U. Daniel, Appl. Phys. Lett. **42**, 137 (1983).

[4] V. I. Denisov, V. F. Zakhar'yash, V. M. Klement'ev and S. V. Chepurov, Instrum. Exp. Tech. **50**, 517 (2007).

[5] K. M. Evenson, D. A. Jennings, and F. R. Petersen, Appl. Phys. Lett. **44**, 576 (1984).

[6] D. Etor, L. E. Dodd, D. Wood and C. Balocco, IEEE Trans. Electron Devices **63**, 2887 (2016).

[7] T Kawanagoa, and S. Oda, Appl. Phys. Lett. **108**, 041605 (2016).

[8] M. Rittner, M. S. Martin-Gonzalez, A. Flores, H. Schweizer, F. Effenberger, and M. H. Pilkuhn, J. Appl. Phys. **98**, 054312 (2005).

[9] Y. He, and J. Kanicki, Appl. Phys. Lett. **76**, 661 (2000).

[10] M. W. Rowell, M. A. Topinka, M. D. McGehee, H. Prall, G. Dennler, N. S. Sariciftci, L. Hu and G. Gruner, Appl. Phys. Lett. **88**, 233506 (2006).

[11] J. Kim, J. Hwang, K. Song, N. Kim, J. C. Shin, and J. Lee, Appl. Phys. Lett. **108**, 253101 (2016).

[12] V. P. Verma, S. Das, I. Lahiri, and W. Choi, Appl. Phys. Lett. **96**, 203108 (2010).

[13] S. Mack, M. A. Meitl, A. J. Baca, Z.-T. Zhu, and J. A. Rogers, Appl. Phys. Lett. **88**, 213101 (2006).

[14] S. Steudel, S. D. Vusser, K. Myny, M. Lenes, J. Genoe, and P. Heremans, J. Appl. Phys. **99**, 114519 (2006).

[15] HD MicroSystems. Product Bulletin: PI-2600 Series—Low Stress Polyimides, (2009).

[16] V. Subramanian, P. C. Chang, J. B. Lee, S. E. Molesa, and S. K. Volkman, IEEE Trans. Compon. Packag. Technol, **28**, 1318 (2005).

[17] R. A. Potyrailo, W. G. Morris, T. Sivavec, H. W. Tomlinson, S. Klensmeden, and K. Lindh, Wireless Commun. Mob. Comput. **9**, 1318 (2009).

[18] H. T. Hsu, and T. J. Huang, IEEE Trans. Antennas Propag. **61**, 4852 (2013).

[19] K. Myny, S. Steudel, P. Vicca, J. Genoe, and P. Heremans, Appl. Phys. Lett. **93**, 093305 (2008).

[20] Y. Pan, C. V. Powell, A. M. Song, and C. Balocco, Appl. Phys. Lett. **105**, 253901 (2014).

[21] M. N. Gadalla, M. Abdel-Rahman, and A. Shamim, Sci. Rep. **4**, 1 (2014).

[22] M. R. Abdel-Rahman, B. Monacelli, A. R. Weeks, G. Zummo, and G. D. Boreman, Opt. Eng**. 44(6)**, 066401, (2005).

[23] K. Choi, F. Yesilkoy, G. Ryu, S. H. Cho, N.l Goldsman, M. Dagenais, and M. Peckerar, IEEE Trans. Electron Devices, **58**, 3519 (2011).

[24] D. M. Pozar, *Oscillators and mixers in Microwave Engineering*, 4th ed. New York, NY, USA: Wiley, 2011, pp. 617–622.

[25] L. E. Dodd, A. J. Gallant, and D. Wood, IEEE sens. conf. **10**, 176 (2011).

[26]T. Königer, Eur. Microelectron. Packag. Conf. **20**, 1 (2015).

[27]R. Zoberbier, M. Hennemeyer, D. Toennies, A. Kraft, M. Eisner, and R. Volkel, Electron. Syst-Integr. Technol. Conf. **3**, 1 (2010).
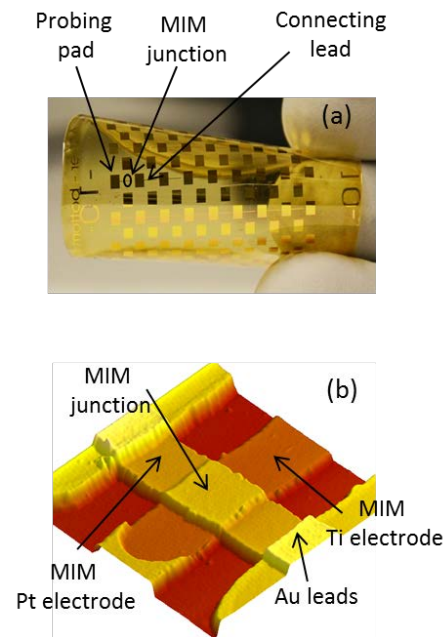
FIGURES

FIG. 1. Picture of fabricated Ti/OTS/Pt devices on PI substrate (a), with the devices' connecting leads and probing pads visible, and (b) an AFM image of one of the devices with the crossover at the middle denoting the diode junction.
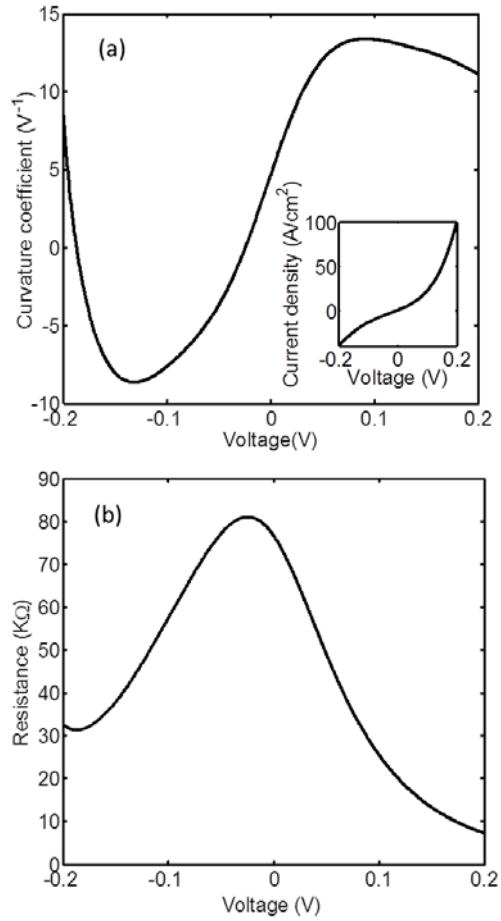
FIG. 2. Typical zero bias curvature coefficient (a), and (b) resistance of the Ti/OTS/Pt device. In the inset is the diode *J-V* characteristic of the diode. The first and second derivatives of the *I-V* were obtained from the result of a 9th order polynomial fitted to the devices' raw *I-V* data.
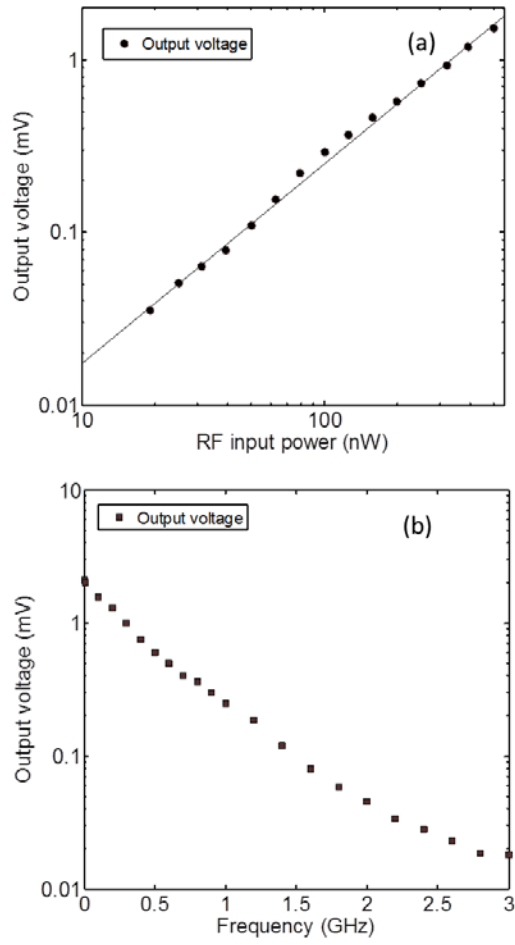
FIG. 3. (a) Rectified voltage as a function of input HF power at a frequency of 1 GHz. (b) Rectified voltage as a function of the frequency. The input power was kept constant at approximately 100 nW (-40 dBm).
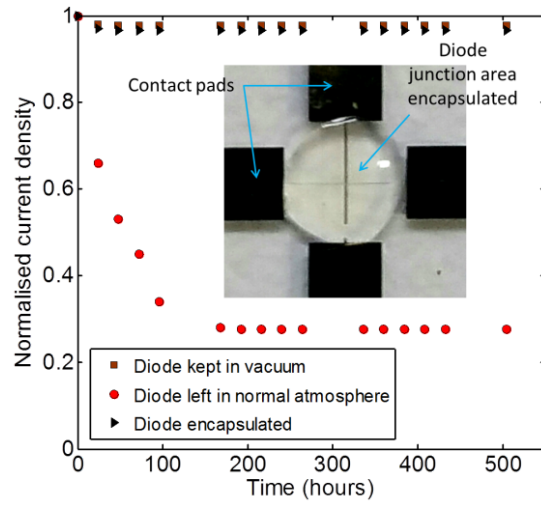
FIG. 4. A typical normalized current density of a Ti/OTS/Pt diode kept in vacuum, normal atmosphere, and encapsulated. In the inset is an image of an encapsulated diode.
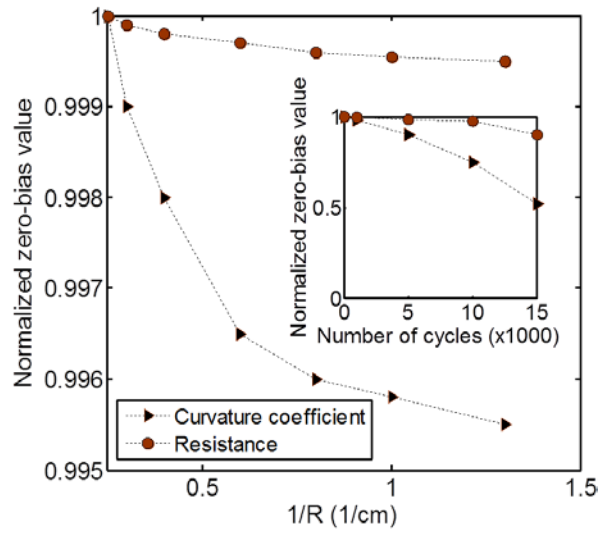
FIG 5. Plot of zero-bias resistance and curvature coefficient of the Ti/OTS/Pt device as a function of substrate curvature. In the inset is the plot of zero-bias resistance and curvature coefficient as a function of bend cycles.